Average bit error rate of multi-hop parallel decode-and-forward-based FSO cooperative system with the max–min criterion under the gamma–gamma distribution

Tian Cao (曹 天)[1], Ping Wang (王 平)[1,2,*], Lixin Guo (郭立新)[2], Bensheng Yang (杨本圣)[1], Jing Li (李 晶)[1], and Yintang Yang (杨银堂)[3]

[1]*State Key Laboratory of Integrated Service Networks, School of Telecommunications Engineering, Xidian University, Xi'an 710071, China*

[2]*School of Physics and Optoelectronic Engineering, Xidian University, Xi'an 710071, China*

[3]*Key Laboratory of the Ministry of Education for Wide Band-Gap Semiconductor Materials and Devices, School of Microelectronics, Xidian University, Xi'an 710071, China*

**Corresponding author: pingwang@xidian.edu.cn*

Received January 28, 2015; accepted May 27, 2015; posted online June 25, 2015

The average bit error rate (BER) performance of a free-space optical (FOS) system based on the multi-hop parallel decode-and-forward cooperative communication method with an M-ary phase shift keying subcarrier intensity modulation is studied systematically. With the max–min criterion as the best path selection scheme, the probability density function and the cumulative distribution function of the gamma–gamma distribution random variable signal-to-noise ratio are derived. The analytical BER expression is then obtained in terms of the Gauss–Laguerre quadrature rule. Monte Carlo simulation is also provided to confirm the validity of the presented average BER model.

OCIS codes: 010.1300, 010.1330, 060.2605, 060.4251.
doi: 10.3788/COL201513.080101.

In recent years, free-space optical (FSO) communication has attracted significant attention due to its very large bandwidth, license-free, excellent security, and being a promising solution for the so-called "last mile" problem[1–6]. However, the existence of atmospheric-induced turbulence will degrade the performance of FSO links particularly with transmission longer than 1 km[7–10]. Viable solutions have been suggested to overcome this problem; for example, partially coherent beam[11], aperture averaging[12], adaptive optics[13], spatial diversity[10], and so on. Among those methods, the spatial diversity technique is especially attractive because of its lower complexity, higher quality of service, power savings, and higher reliability in bit error rate (BER) for FSO systems. Recently, as an important way of realizing spatial diversity advantages, cooperative diversity has been introduced and investigated in FSO communication to mitigate fading over turbulence channels[9,14–16]. In Ref. [9], the outage probability with respect to standalone uses of parallel and multi-hop relaying decode-and-forward (DF) has been studied considering the path-loss and the log-normal (LN) fading commonly used in weak turbulence conditions. In Ref. [14], the BER of the DF protocol in a binary phase shift keying (BPSK) subcarrier intensity modulation (SIM)-based FSO cooperative communication system following the gamma–gamma (G–G) distribution has been derived with only one source, one destination, and one single relay node. In Ref. [15], the average BER performance of a DF system with a parallel relay selection scheme on the basis of the highest instantaneous signal-to-noise ratio (SNR) of the G–G distributed source-relay links has been analyzed. In Ref. [16], the outage performance of selective DF-based FSO mesh networks building upon a combination of multi-hop and parallel relaying over the LN turbulence channel has been investigated. The so-called multi-hop parallel relaying scheme demonstrated substantial performance improvements with respect to both standalone serial and parallel relaying schemes. In fact, the DF system may suffer from the severely erroneous relaying of the data from relays. To solve this problem, an optimal relay selection scheme can be adopted to enhance the system performance. Normally, the best relay is selected based on the highest value of the minimum of source-to-relay, relay-to-relay, and relay-to-destination SNR, which is known as the max–min criterion-based path selection scheme[17]. Thus, it is necessary to study the multi-hop parallel DF-based FSO cooperative system with the max–min criterion under G–G distributed fading channels for applications. However, there are no such works published in the context of FSO system to date, to the best of our knowledge.

In this work, the BER performance of multi-hop parallel DF-based FSO cooperative communication system over a G–G turbulence fading channel has been investigated with the max–min criterion as the best path selection scheme. The probability density function (PDF) and cumulative distribution function (CDF) of a random variable (RV)

obeying the max–min G–G distribution with regards to the SNR has been derived for the first time, to our best knowledge. The BER of a symbol-wise multi-hop parallel DF system over G–G channels with M-ary phase-shift keying (MPSK) modulation is further achieved based on the Gauss–Laguerre quadrature rule, which is verified by Monte Carlo (MC) simulation. For simplicity, the effect of pointing errors has not been considered.

Figure 1 shows an MPSK modulated cooperative communication system based on the symbol-wise DF with R parallel paths between the source and destination nodes. A total of C hops are assumed to be in the cooperative path; that is, there are $C-1$ relays in each path. As known, the relays may commit error when they decode the data from the previous node. In the chosen cooperative path, the relays utilize a symbol-wise DF method to demodulate the data transmitted from the previous node. Only one relay can be allowed to pass the data to the next node at one time without using error correction coding and error detection coding. A direct path of source-to-destination (SD) is also considered in our work. In each link, the received electrical signal ($y_{m,n}$) can be expressed as[18]

$$y_{m,n} = R_p h_{m,n} x_{m,n} + n_{m,n}, \tag{1}$$

where $m = 1, ..., R$ and $n = 1, ..., C$. Term R_p is the detector responsivity, $h_{m,n}$ is the normalized channel fading coefficient obeying the G–G distribution, $x_{m,n}$ represents the transmitted data, and $n_{m,n}$ is the zero-mean additive white Gaussian noise (AWGN) with variance $\sigma_n^2 = N_0/2$ in each link.

As known, the PDF of the G–G distribution is given in Refs. [19,20] as

$$f_{h_{m,n}}(h) = \frac{2(\alpha\beta)^{(\alpha+\beta)/2}}{\Gamma(\alpha)\Gamma(\beta)} h^{(\alpha+\beta)/2-1} K_{\alpha-\beta}[2(\alpha\beta h)^{1/2}], \tag{2}$$

where $\Gamma(\cdot)$ is the gamma function, and $K_v(\cdot)$ is the second kind of modified Bessel function of order v. Terms α and β are the shape parameters of the G–G variable, and they are related to physical FSO system parameters via the Rytov variance σ_R^2 as follows[19,21]

$$\alpha = \{\exp[0.49\sigma_R^2/(1+1.11\sigma_R^{12/5})^{7/6}] - 1\}^{-1}, \tag{3}$$

$$\beta = \{\exp[0.51\sigma_R^2/(1+0.69\sigma_R^{12/5})^{5/6}] - 1\}^{-1}, \tag{4}$$

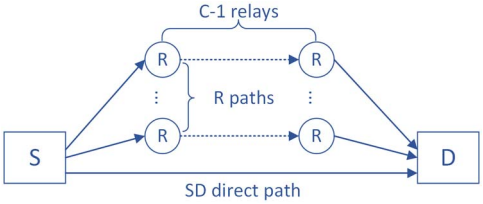

Fig. 1. Structure of our multi-hop parallel DF communication system.

where $\sigma_R^2 = 1.23 C_n^2 k^{7/6} L^{11/6}$, $k = 2\pi/\lambda$ is the wave number, λ is the wavelength, and L is the propagation distance.

The received electrical SNR $\gamma_{m,n}$ in each link can be expressed as $\gamma_{m,n} = (R_p h_{m,n})^2/N_0$. Considering that the G–G distribution is normalized, the corresponding average electrical SNR can be obtained as $\bar{\gamma}_{m,n} = R_p^2/N_0$. Thus, the PDF and CDF of RV $\gamma_{m,n}$ can be written as

$$f_{\gamma_{m,n}}(\gamma) = \frac{B}{4} A_{m,n}^{\alpha+\beta} \gamma^{\frac{\alpha+\beta-4}{4}} K_{\alpha-\beta}(A_{m,n}\gamma^{1/4}), \tag{5}$$

$$F_{\gamma_{m,n}}(\gamma) = B \int_0^{A_{m,n}\gamma^{1/4}} x^{(\alpha+\beta-1)} K_{\alpha-\beta}(x)\mathrm{d}x, \tag{6}$$

where $A_{m,n} = \sqrt{4\alpha\beta/\sqrt{\bar{\gamma}_{m,n}}}$ and $B = 2^{(2-\alpha-\beta)}/(\Gamma(\alpha)\Gamma(\beta))$.

According to Ref. [22, Eq. (14)], and Ref. [23], the CDF of $\gamma_{m,n}$ can be simplified as

$$F_{\gamma_{m,n}}(\gamma) = B \cdot 2^{\alpha+\beta-2} G_{1,3}^{2,1}\left(\frac{A_{m,n}^2}{4}\gamma^{1/2}\middle| \begin{matrix} 1 \\ \alpha, \beta, 0 \end{matrix}\right), \tag{7}$$

where $G_{p,q}^{m,n}(\cdot)$ is the Meijer-G function.

Considering the aforementioned DF communication system, $\gamma_{m,n}$ can be further considered as an $R \times C$ matrix. Then, defining a RV $\gamma_{\max,\min}$ based on the max–min criterion, the $\gamma_{\max,\min}$ is given in Ref. [17] as

$$\gamma_{\max,\min} = \max(\min(\gamma_{m,n})|_{n=1}^{C})|_{m=1}^{R}. \tag{8}$$

It is known from Eq. (8) that the minimum $\gamma_{m,n}$ of each row is achieved first and then the maximum value of these lowest-value $\gamma_{\max,\min}$ can be selected.

Assuming $\bar{\gamma}_{m,n} = \bar{\gamma}_{s,d} = \bar{\gamma}$, where $\bar{\gamma}_{s,d}$ is the average SNR for the SD path, it can be known that $A_{m,n}$ is the same in each link; let it equal A ($A_{m,n} = A = \sqrt{4\alpha\beta/\sqrt{\bar{\gamma}}}$). Thus, Eqs. (5) and (7) can be rewritten as

$$\hat{f}_{\gamma_{m,n}}(\gamma) = \frac{B}{4} A^{\alpha+\beta} \gamma^{\frac{\alpha+\beta-4}{4}} K_{\alpha-\beta}(A\gamma^{1/4}), \tag{9}$$

$$\hat{F}_{\gamma_{m,n}}(\gamma) = B \cdot 2^{\alpha+\beta-2} G_{1,3}^{2,1}\left(\frac{A^2}{4}\gamma^{1/2}\middle| \begin{matrix} 1 \\ \alpha, \beta, 0 \end{matrix}\right). \tag{10}$$

Then, the CDF of $\gamma_{\max,\min}$ can be derived based on Eqs. (8) and (10), Ref. [24, Eqs. [(6-54) and (6-56)] as follows

$$F_{\gamma_{\max,\min}}(\gamma) = \{1 - [1 - \hat{F}_{\gamma_{m,n}}(\gamma)]^C\}^R. \tag{11}$$

Then, the PDF of $\gamma_{\max,\min}$ can be obtained by differentiating Eq. (11) with respect to γ, as follows

$$f_{\gamma_{\max,\min}}(\gamma) = RC \cdot \{1 - [1 - \hat{F}_{\gamma_{m,n}}(\gamma)]^C\}^{R-1} \times [1 - \hat{F}_{\gamma_{m,n}}(\gamma)]^{C-1} \hat{f}_{\gamma_{m,n}}(\gamma). \tag{12}$$

Let $\gamma_{s,d}$ denote the instantaneous SNR of the SD direct path. From Eq. (10), the CDF of it can be written as

$$F_{\gamma_{s,d}}(\gamma) = B \cdot 2^{\alpha+\beta-2} G_{1,3}^{2,1}\left(\frac{A^2}{4}\gamma^{1/2}\middle| \begin{matrix} 1 \\ \alpha,\beta,0 \end{matrix}\right). \tag{13}$$

For the system studied, the best path should include the $\gamma_{\max,\min}$. For the SD direct path, the following selection scheme can be used

$$\begin{matrix} \text{if } \gamma_{\max,\min} > \gamma_{s,d}, & \text{using cooperative path} \\ \text{if } \gamma_{s,d} > \gamma_{\max,\min}, & \text{using SD path.} \end{matrix} \tag{14}$$

In accordance with Eq. (14), a new RV $\gamma_{\max}$ is defined as follows

$$\gamma_{\max} = \max(\gamma_{\max,\min}, \gamma_{s,d}). \tag{15}$$

The CDF of RV $\gamma_{\max}$ can be written as[24]

$$\begin{aligned} F_{\gamma_{\max}}(\gamma) &= F_{\gamma_{\max,\min}}(\gamma) \cdot F_{\gamma_{s,d}}(\gamma) \\ &= \left\{1 - \left[1 - B \cdot 2^{\alpha+\beta-2} G_{1,3}^{2,1}\left(\frac{A^2}{4}\gamma^{1/2}\middle| \begin{matrix} 1 \\ \alpha,\beta,0 \end{matrix}\right)\right]^C\right\}^R \\ &\quad \times B \cdot 2^{\alpha+\beta-2} G_{1,3}^{2,1}\left(\frac{A^2}{4}\gamma^{1/2}\middle| \begin{matrix} 1 \\ \alpha,\beta,0 \end{matrix}\right), \end{aligned} \tag{16}$$

and the PDF of RV $\gamma_{\max}$ can be obtained from Eq. (16) as follows

$$\begin{aligned} f_{\gamma_{\max}}(\gamma) &= \left[\frac{B}{4} A^{\alpha+\beta} \gamma^{\frac{\alpha+\beta-4}{4}} K_{\alpha-\beta}(A\gamma^{1/4})\right] \\ &\quad \times \{[1 - (1 - \hat{F}_{\gamma_{m,n}}(\gamma))^C]^R + RC \cdot \hat{F}_{\gamma_{m,n}}(\gamma) \\ &\quad \cdot [1 - (1 - \hat{F}_{\gamma_{m,n}}(\gamma))^C]^{R-1} \cdot (1 - \hat{F}_{\gamma_{m,n}}(\gamma))^{C-1}\}. \end{aligned} \tag{17}$$

Considering the difficulty in determining the accurate end-to-end SNR of our DF system, $\gamma_{\max}$ is adopted as the approximate end-to-end SNR[17]. As known, the BER of an MPSK over an AWGN channel can be written as[25]

$$p_e(\gamma) = D(M) \cdot \operatorname{erfc}\left(\sqrt{\gamma}\,\sin\frac{\pi}{M}\right), \tag{18}$$

where $D(M) = 1/\max(\log_2 M, 2)$ and $\operatorname{erfc}(\cdot)$ is the complementary error function. Thus, the approximate average BER of an MPSK-based multi-hop parallel DF system with the best path selection scheme over a G–G fading channel can be obtained from Eqs. (16)–(18) as

$$\begin{aligned} P_e &= \int_0^\infty p_e(\gamma) \times f_{\gamma_{\max}}(\gamma)\mathrm{d}\gamma \\ &= \frac{D(M)}{\sqrt{\pi}} \int_0^\infty \gamma^{-1/2} e^{-\gamma} F_{\gamma_{\max}}\left(\frac{\gamma}{\sin^2(\pi/M)}\right)\mathrm{d}\gamma. \end{aligned} \tag{19}$$

The Gauss–Laguerre quadrature rule[26] can be used to efficiently and accurately approximate Eq. (19). Thus Eq. (19) can be written as

$$P_e \approx \frac{D(M)}{\sqrt{\pi}} \sum_{k=1}^{n} Y_k F_{\gamma_{\max}}\left(\frac{x_k}{\sin^2(\pi/M)}\right), \tag{20}$$

where $F_{\gamma_{\max}}(\gamma)$ is given in Eq. (16), x_k is the kth root of the generalized Laguerre polynomial $L_n^{(-1/2)}(x)$, and the weight Y_k can be calculated by[27]

$$Y_k = \frac{\Gamma(n+1/2)x_k}{n!(n+1)^2[L_{n+1}^{(-1/2)}(x_k)]^2}. \tag{21}$$

The analytical results in this paper are obtained from Eq. (20). Term n is chosen to be 30 in computing the generalized Gauss–Laguerre approximations. In accordance with Eqs. (3) and (4), $(\alpha,\beta) = (6.0, 4.4)$, (4.0,1.9), and (4,2,1.4) are adopted in this work, corresponding to the G–G shape parameters in weak turbulence ($\sigma_R^2 = 0.5$), moderate turbulence ($\sigma_R^2 = 1.6$), and strong turbulence ($\sigma_R^2 = 3.5$), respectively.

Figure 2 shows the average BER of the DF system with max–min criterion as the best path selection scheme over G–G fading channel at different SNRs, which contains two cooperative paths (three hops in each path) and a SD direct path. The modulation type includes BPSK, QPSK, 8PSK, and 16PSK modulations. It is seen from Fig. 2 that the analytical results have excellent agreement with the MC simulations. This confirms the accuracy of our BER model. It is also found that the BER of the system increases with the increase of the value of Rytov variance (from weak to strong turbulence). For example, when the SNR is equal to 20 dB, the average BERs of BPSK modulation are 10^{-6}, 10^{-4}, and 10^{-3} in weak, moderate, and strong turbulence conditions, respectively. It is obvious that the BER value increases with the increase of M-ary.

In Fig. 3, the analytical and simulated BER of a BPSK modulated DF system with $R = 2$ and $C = 6$ using the best path selection scheme has been plotted. For comparison, the simulated BER using the random path selection scheme is also given. It can be found from Fig. 3 that the BER performance of the best path selection scheme is significantly superior to that of the random path selection scheme. For instance, when the SNR is equal to 40 dB, the average BER of the random path selection scheme is 10^{-3}, whereas the average BER of the best path scheme is 10^{-8} in the moderate turbulence condition. Moreover, the relative diversity order (RDO) for this scenario can be also achieved based on our analytical results shown in Fig. 3 using Ref. [28, Eq. (50)] . Taking the random path selection scheme as a benchmark, according to the results shown in Fig. 3, the RDO for the best path selection scheme-based DF system with two parallel cooperative paths is approximately 2 in the three turbulence conditions as the SNR trends to infinity.

In Fig. 4, the analytical and simulated BER of BPSK modulation versus the SNR with the same number of relays in each path but a different number of cooperative paths is shown. The solid lines represent the DF system with five cooperative paths and three hops in each path. The dash–dot lines represent the DF system with two cooperative paths and three hops in each path. It is found that the BER value decreases with an increasing number

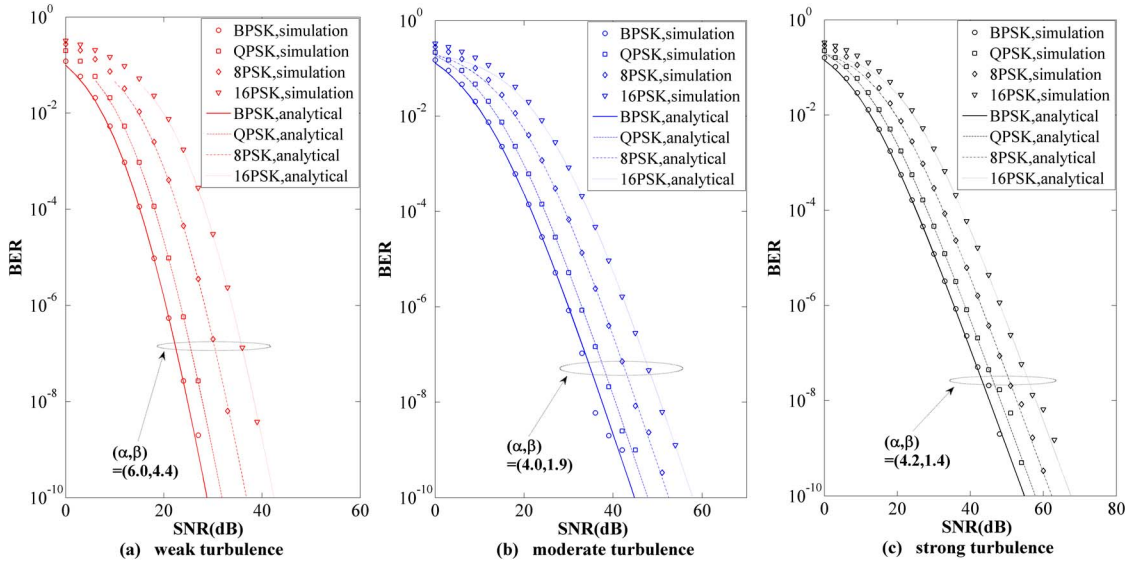

Fig. 2. BER performance of our DF system with $R = 2$ and $C = 3$ in (a) weak, (b) moderate, and (c) strong turbulence conditions using BPSK, QPSK, 8PSK, and 16PSK modulations.

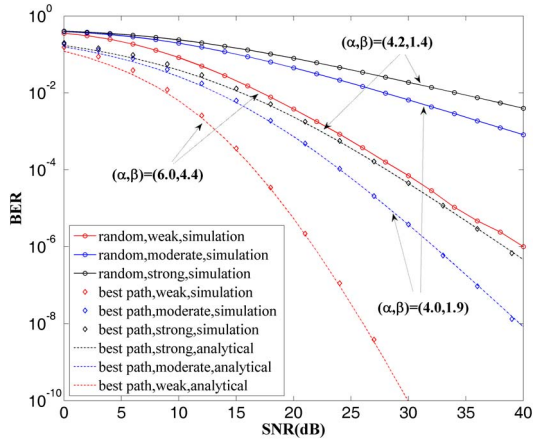

Fig. 3. BER performance of our multi-hop parallel DF system with the best path selection and random path selection-based schemes using BPSK modulation.

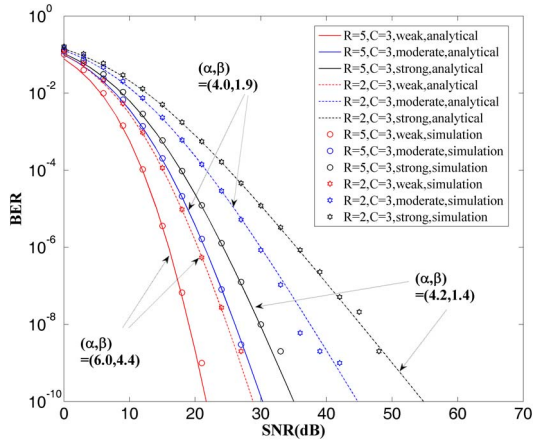

Fig. 4. BER comparison of $R = 2$ and $C = 3$ with that of $R = 5$ and $C = 3$ in weak, moderate, and strong turbulence conditions.

(R) of cooperative paths. For example, when the SNR is equal to 20 dB, the BERs of the studied system with $R = 2$ and $C = 3$ are 10^{-6}, 10^{-4}, and 10^{-3} in weak, moderate, and strong turbulence conditions, respectively, whereas the BERs of $R = 5$ and $C = 3$ are 10^{-9}, 10^{-6}, and 10^{-5} in weak, moderate, and strong turbulence conditions, respectively. This is because adding more cooperative paths in the DF system can improve the diversity gain.

In conclusion, a generalized multi-hop parallel FSO system over G–G fading channels with a DF relaying protocol is presented, the structure of which can be adjusted by changing the structure parameters R and C. Based on it, the max–min criterion is adopted as the best path selection scheme to improve the system performance. The analytical expression of the average BER for MPSK modulation is derived in terms of the Gauss–Laguerre quadrature rule. MC simulations confirm the validity of the analytical results. The theoretical study shows that the performance of the present system can be improved effectively by the max–min criterion. Furthermore, increasing the number of parallel cooperative paths (R) in the current system can achieve better diversity gain to mitigate the degrading effects of turbulence-induced fading. This work will be of help for the system design of MPSK SIM-based FSO systems employing the DF cooperative scheme.

This work was supported by the National Natural Science Foundation of China (No. 61474090), the Natural Science Basic Research Plan in Shaanxi Province of China (No. 2014JM8340), the China Postdoctoral Science Special Foundation (No. 201104659), the China Postdoctoral Science Foundation (No. 20100481322), and the Fundamental Research Funds for the Central Universities (No. NSIY041404). This work was also partly supported by the 111 Project of China (No. B08038).

References

1. P. Butala, H. Elgala, and T. D. C. Little, Chin. Opt. Lett. **12**, 090602 (2014).
2. J. Xiao, C. Tang, X. Li, J. Yu, X. Huang, C. Yang, and N. Chi, Chin. Opt. Lett. **12**, 050603 (2014).
3. N. D. Chatzidiamantis, D. S. Michalopoulos, E. E. Kriezis, G. K. Karagiannidis, and R. Schober, J. Opt. Commun. Netw. **5**, 92 (2013).
4. C. Abou-Rjeily and S. Haddad, IEEE Trans. Commun. **62**, 1970 (2014).
5. X. Tang, Z. Wang, Z. Xu, and Z. Ghassemlooy, J. Lightw. Technol. **32**, 2597 (2014).
6. J. M. Garrido-Balsells, A. Jurado-Navas, J. F. Paris, M. Castillo-Vázquez, and A. Puerta-Notario, Opt. Lett. **38**, 3984 (2013).
7. J. C. Juarez, D. M. Brown, and D. W. Young, Opt. Express **22**, 12551 (2014).
8. F. Tang and B. Zhu, Chin. Opt. Lett. **11**, 090101 (2013).
9. M. Safari and M. Uysal, IEEE Trans. Wireless Commun. **7**, 5441 (2008).
10. K. P. Peppas, F. Lazarakis, A. Alexandridis, and K. Dangakis, Opt. Lett. **37**, 3243 (2012).
11. O. Koroktova, L. C. Andrews, and R. L. Phillips, Opt. Eng. **43**, 330 (2004).
12. L. C. Andrews and R. L. Phillips, *Laser Beam Propagation through Random Media* (SPIE, 2005).
13. R. K. Tyson, J. Opt. Soc. Am. A **19**, 753 (2002).
14. M. R. Bhatnagar, IEEE Photon. Technol. Lett. **24**, 545 (2012).
15. M. R. Bhatnagar, in *2013 IEEE International Conference on Communications (ICC)* 3142 (2013).
16. M. A. Kashani and M. Uysal, J. Opt. Commun. Netw. **5**, 901 (2013).
17. M. R. Bhatnagar, IEEE Commun. Lett. **16**, 1980 (2012).
18. X. Yi, Z. Liu, and P. Yue, Opt. Lett. **38**, 208 (2013).
19. A. Al-Habash, L. C. Andrews, and R. L. Phillips, Opt. Eng. **40**, 1554 (2001).
20. P. Puri, P. Garg, and M. Aggarwal, IEEE Photon. Technol. Lett. **26**, 1797 (2014).
21. R. Boluda-Ruiz, A. García-Zambrana, C. Castillo-Vázquez, and B. Castillo-Vázquez, Opt. Express **22**, 16629 (2014).
22. V. S. Adamchik and O. I. Marichev, in *Proceedings of the International Symposium on Symbolic and Algebraic Computation* 212 (1990).
23. Wolfram, The Wolfram Functions Site, http://functions.wolfram.com/07.34.21.0002.01 (October 29, 2001).
24. A. Papoulis, *Probability, Random Variables, and Stochastic Processes* (McGraw–Hill, 1991).
25. P. Wang, L. Zhang, L. Guo, F. Huang, T. Shang, R. Wang, and Y. Yang, Opt. Express **22**, 20828 (2014).
26. P. Concus, D. Cassatt, G. Jaehnig, and E. Melby, Math. Comput. **17**, 245 (1963).
27. W. H. Press, S. A. Teukolsky, W. T. Vetterling, and B. P. Flannery, *Numerical Recipes in C: The Art of Scientific Computing* (Cambridge University, 1992).
28. M. Safari and M. Uysal, IEEE Trans. Wireless Commun. **7**, 1963 (2008).